Meas. Sci. Technol. 5 (1994) 1124–1130. Printed in the UK

Cut-off wavelength measurements of Ti : $LiNbO_3$ channel waveguides

T Lang, L Thévenaz, Z B Ren and Ph Robert

Swiss Federal Institute of Technology (EPFL), Laboratory of Metrology, CH-1015 Lausanne, Switzerland

Received 20 July 1993, in final form 1 March 1994, accepted for publication 19 May 1994

Abstract. One of the most important parameters in characterization of integrated optical devices is precise determination of the effective cut-off wavelength of the fundamental and first-order modes, since this sets the exact region of single-mode operation. This paper describes an experimental set-up for determination of cut-off wavelengths of integrated optical waveguides, using the technique of spectral light transmission. Measurement results obtained with Ti : $LiNbO_3$ channel waveguides are presented for straight waveguides, bent waveguides and polarizers.

1. Introduction

The theoretical values for cut-off wavelengths of guided modes can be obtained by rigorously solving the wave equations, taking into account the refractive index profile and the geometrical structure of the waveguide. However, calculations for arbitrary waveguides are very complicated and only appropriate for straight-channel waveguides. In bent waveguides, the effective measured cut-off wavelengths can shift to considerably shorter wavelengths, due to increasing attenuation losses as the wavelength approaches the theoretical cut-off wavelength.

Therefore, experimentally observed effective cut-off wavelengths are of far greater importance for practical use. They strongly depend on waveguide geometry, launching conditions and the measurement technique itself [1–4]. It is convenient to define the effective cut-off wavelength for a certain mode as the wavelength at which this mode is practically absent at the exit of the waveguide [5].

For measurements of cut-off wavelengths of optical fibres, two standard reference test methods based on spectral light transmission techniques are recommended by international standard organizations such as the CCITT. These are the single-bend and power-step techniques [4–6]. The latter is also well suited to measurements of cut-off wavelengths of channel waveguides [7, 8]. We used an improvement of this technique, which allows better mode excitation and extended the cut-off wavelength measurements to bent waveguides and polarizers.

The problems faced in measuring effective cut-off wavelengths of short and not pigtailed integrated optical devices are still more delicate to overcome than those for optical fibres. Proper excitation of waveguides is essential for their correct characterization. On the one hand it has to be ensured that the incoherent light source is exciting all possible modes with the same amount of power. Therefore, the light spot at the entrance of the waveguide should be larger than the strip waveguide width. On the other hand, the light spot should be sufficiently confined to prevent too much light being injected into the substrate, thus exciting unwanted substrate radiation modes. Furthermore, at the cut-off wavelength of a mode, the whole energy of the no-longer-guided mode is transferred into substrate radiation and leaky modes.

All these radiation modes propagate along the waveguide. They will continuously lose power along the propagation direction, since they are 'leaking' into the substrate. Owing to the small length of the waveguide, they can still play an important role at the exit of the waveguide and provide biased measurements.

2. The experimental set-up

Figure 1 shows the experimental set-up. The image of the linearly polarized light from a halogen white light source is first projected onto the plane of an aperture (diameter 100 μm) with a pair of lenses. The aim of the aperture was to select only a small part of the coiled filament to ensure a more uniform and limited illumination of the integrated optical device than is possible with the systems presented in [7, 8]. With the help of this aperture, the spot size of the launching light beam was sufficiently reduced (to 20 μm) to accomplish efficient light injection into the waveguide without too much light being lost into the substrate. A high-quality lens such as a microscope objective focuses the image of the source aperture onto the waveguide. The numerical aperture of the microscope (NA = 0.35) was chosen to be high enough to excite all possible guided modes.

0957-0233/94/091124+07 $19.50

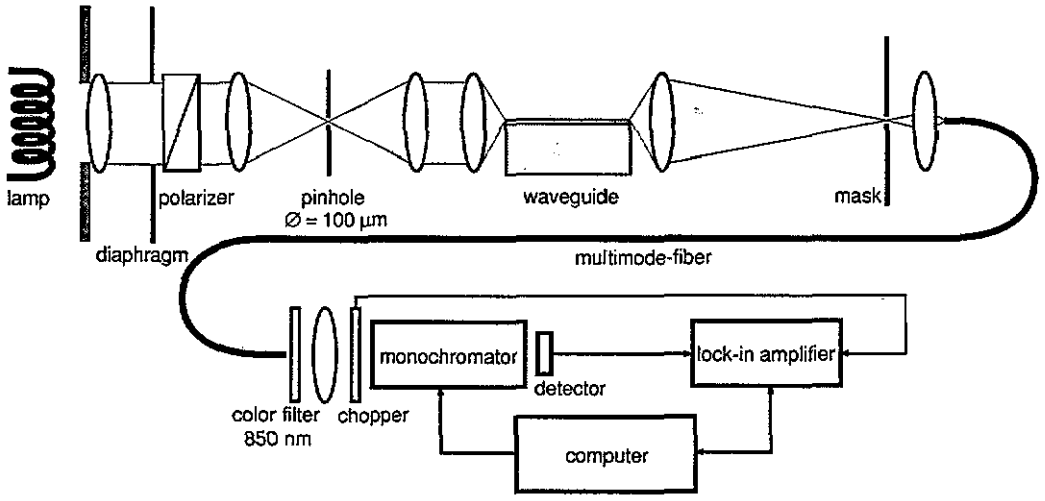

Figure 1. The experimental set-up for cut-off wavelength measurements.

The image of the output light of the waveguide is focused onto the face of a multimode fibre. A prefixed adjustable aperture mask (spatial filter) enables precise injection of the light coming from the waveguide into the multimode fibre. It also eliminates the leakage light. The fibre output is then directed into a monochromator, after it passes through a chopper and a colour filter. The spectral resolution of the monochromator was chosen to be 5 nm and scanned in the desired wavelength region 900–1600 nm. The spectrally filtered light at the exit slit of the monochromator is detected by an InGaAs detector, the signal is then amplified by a lock-in amplifier.

Contrary to the systems presented in [7, 8], the arrangement of the monochromator behind the waveguide facilitates light injection into the correct waveguide of the sample (the entrance light spot is visible under a microscope). In the same way, light injection into a multimode fibre is made easier, since more power is available.

Adjustment of the whole system for light injection and light recovery had always been effected at $\lambda =$ 1100 nm. With this adjustment wavelength, the transmission steps in the spectrum were clearly visible for the shorter wavelengths of interest (900–1400 nm). We also noticed that the choice of adjustment wavelength had no influence on the cut-off positions.

To eliminate the spectral response of the launch and detection components of the system (such as the broadband lamp, the detector and the monochromator), the spectral output power $P(\lambda)$ had to be normalized. The best results as a reference power spectrum $P_r(\lambda)$ were achieved by measuring the optical output power spectrum of the whole system without the waveguide. This normalization also minimizes the effects of chromatic aberrations of the microscope lenses. The ratio between $P(\lambda)$ and $P_r(\lambda)$, the normalized transmission spectrum

$$r(\lambda) = 10 \log\left(\frac{P(\lambda)}{P_r(\lambda)}\right)$$

is then plotted as a function of wavelength.

3. Examined components

We examined the following different types of Ti : $LiNbO_3$ channel waveguides for both TE and TM mode excitation: straight waveguides, straight waveguides with polarizers and bent waveguides. The components were X-cut and with y or z propagation.

Figure 2 gives a typical example of the obtained normalized output spectra for straight waveguides with three different strip widths. The cut-off wavelengths can be determined from these figures. The cut-off wavelength for the fundamental mode (λ_{c00}) is defined to be the point at which the transmission spectrum drops by 3 dB after having attained its last maximum (point B). The cut-off wavelength for the first-order mode (λ_{c01}) is defined as the point at which the normalized transmission spectrum starts to rise again (point A, in accordance with [7, 8]).

In figure 3, the variation of the cut-off wavelengths of fundamental and first-order modes as a function of the Ti strip width is summarized. From figure 3, the single-mode region for each waveguide width can be identified with reasonable precision adequate for practical purposes.

To confirm measurement repeatability in terms of cut-off position and transmission levels, some waveguides were measured several times. Figure 4 gives an example of a waveguide for which the measurements were repeated five times. The graph shows that the cut-off wavelength for the first-order mode ($\lambda_{c01} = 1130$ nm) could be reproduced with good consistency in all five measurements (a precision of about 10 nm could be obtained), whilst the variation of spectral power transmission due to chromatic aberrations becomes more important as wavelength increases. At the upper limit of the measured spectral range (1600 nm), the spectral transmission power varied by up to 2 dB, depending on the measurement. The reproducibility in determination of cut-off wavelengths could also be maintained in regions where the power levels were fluctuating.

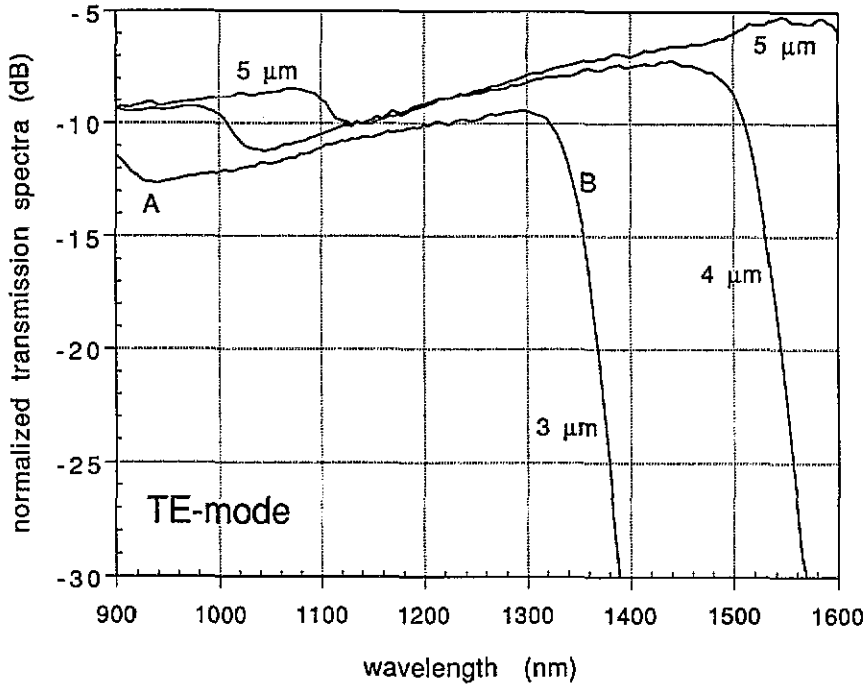

Figure 2. Typical normalized transmission spectra for straight waveguides with different strip waveguide width. Fabrication parameters are Ti thickness 780 Å, diffusion temperature 1020 °C, diffusion time 9 h, waveguide length 40 mm, X-cut and *z* propagation.

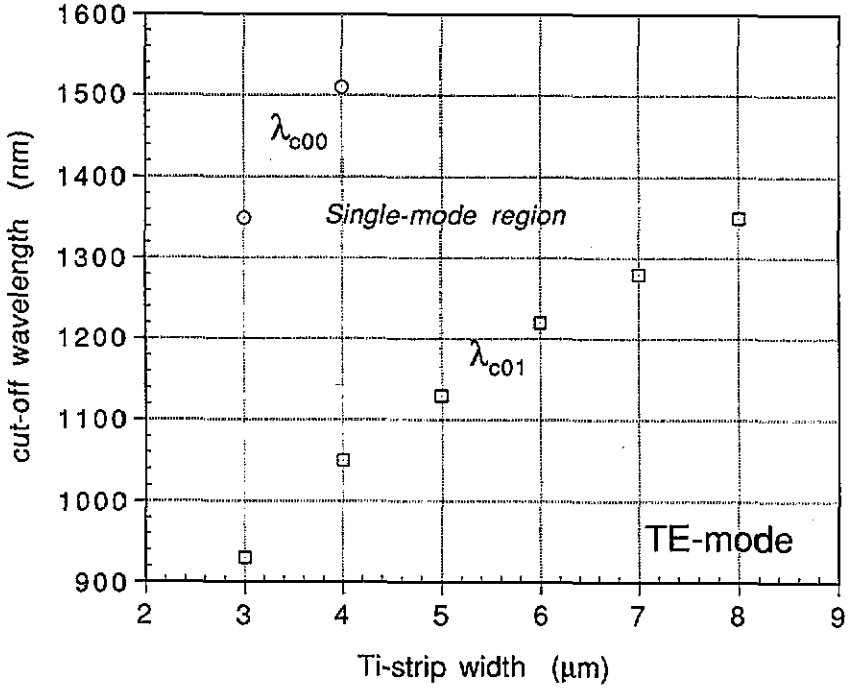

Figure 3. Variation of cut-off wavelengths of the fundamental (λ_{c00}) and first-order (λ_{c01}) modes as a function of Ti strip width.

It can therefore be concluded that the presented system gives very good reproducibility in determination of cut-off wavelengths, whilst the relative value of the spectral transmission power can only be obtained with rough precision for longer wavelengths (that is, for wavelengths greater than 1400 nm, a precision of about 2 dB is obtained).

The strong dependence of cut-off wavelengths on strip waveguide width was verified. For wider strip widths w, they shifted at a rate of $\Delta\lambda/\Delta w \approx 50$–

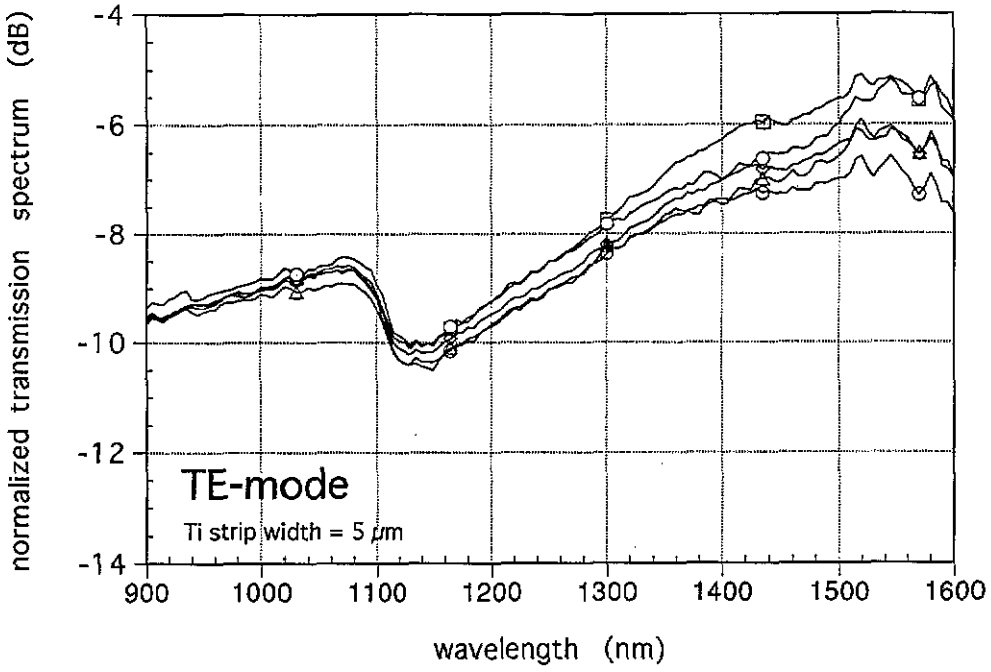

Figure 4. Measurement reproducibility: the same waveguide measured five times. Fabrication parameters are Ti thickness 780 Å, Ti strip waveguide width 5 μm, diffusion temperature 1020 °C, diffusion time 9 h, waveguide length 40 mm, X-cut and *z* propagation.

150 nm μm^{-1} to higher wavelengths, depending on the examined components.

The curved waveguides (see figure 5) consisted of two offset parallel waveguides, where the transition region connecting the two waveguides was specified by the following formula [9], where l_x denotes longitudinal separation in the x direction and l_y lateral offset in the y direction:

$$y=\frac{l_y}{l_x}x-\frac{l_y}{2\pi}\sin\left(2\pi\frac{x}{l_x}\right).$$

The radius of curvature of the bending section changes according to the given sine-wave function to minimize mode conversion loss due to optical field mismatch.

The transmission spectra of bent waveguides showed (figure 5) that the bends were leading to a downshift of cut-off wavelength with decreasing curvature radius. It could also be stated that decreasing the curvature radii of the bent waveguides was reducing their single-mode region. Compared with the reference straight waveguide (with a cut-off wavelength $\lambda_{c01(ref)}=1180$ nm, see figure 5), we obtained for the waveguide with a longitudinal offset of 3 mm a downshift of the cut-off wavelength of the first-order mode of $\Delta\lambda_{c01}=-190$ nm (to a value of $\lambda_{c01(3\text{ mm})}=990$ nm), the single-mode region becoming smaller from 500 nm for a longitudinal separation of $l_x=6$ mm (with cut-off wavelengths $\lambda_{c00(6\text{ mm})}=1600$ nm and $\lambda_{c01(6\text{ mm})}=1100$ nm respectively) to 430 nm for $l_x=3$ mm (with $\lambda_{c00(3\text{ mm})}=1420$ nm).

In the same way, the bends were leading to supplement radiation losses, that became more important for the fundamental mode near its cut-off wavelength and for smaller curvature radii. According to figure 5, an operating wavelength of 1300 nm would cause supplement radiation losses due to bending of about 2 dB for the waveguide of $l_x=3$ mm compared to the straight waveguide.

It is thus very important to optimize the waveguides in a way that the cut-off wavelength for the first-order mode is very close to the later operating wavelength. It can be seen that the supplementary radiation losses due to bending are lowest just above the cut-off wavelength for the first-order mode, due to the very good mode confinement. The waveguide group presented in figure 5 would therefore be ideally suited for an operating wavelength of 1200 nm, thus enabling small longitudinal offsets of $l_x=3$ mm [to become possible without introducing significant supplementary radiation losses.

We also examined the cut-off wavelength behaviour of polarizers. They were fabricated by depositing a low-index buffer and a metal-cladding layer on the waveguides (figure 6). The metal-cladding leads to strong differential absorption of the TE and TM modes. The TM mode is coupled into a highly lossy surface plasmon mode, thus strongly attenuated by the metal. This effect is particularly important at phase-matching between the normal guided wave and the surface plasmon wave. The aim of having a buffer layer of suitable thickness between the waveguide and the metallic layer is to enhance further TM mode attenuation with respect to TE mode attenuation [10].

Figure 6 shows the spectral behaviour of a polarizer for TE and TM mode excitation. The transmission spectrum for TE mode excitation gives cut-off values of $\lambda_{c01}=1010$ nm and $\lambda_{c00}=1420$ nm.

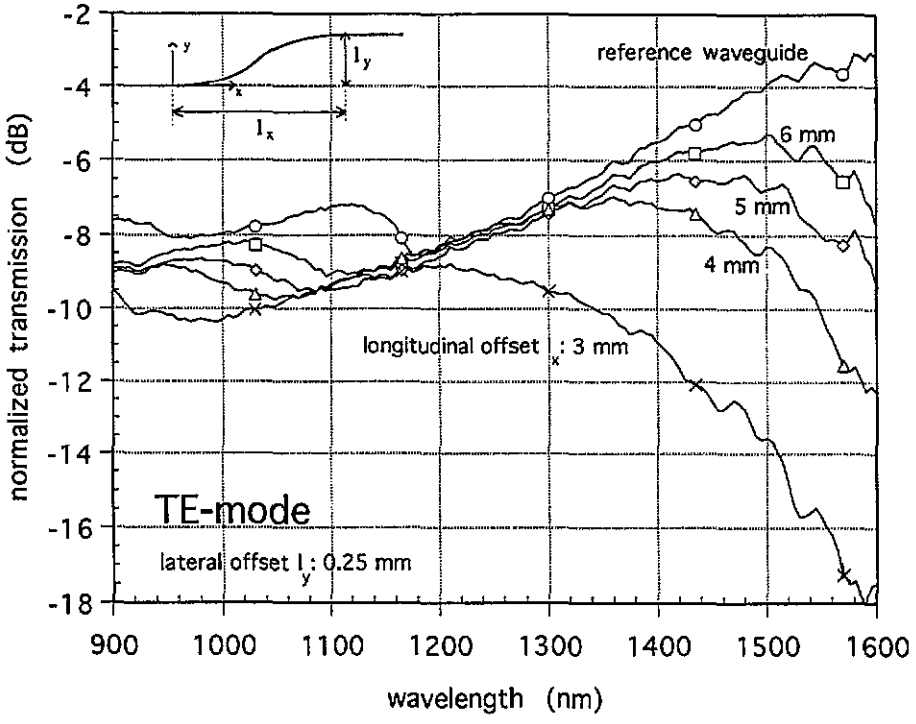

Figure 5. Transmission spectra and waveguide pattern of bent waveguides. Fabrication parameters are Ti thickness 780 Å, Ti strip waveguide width 6 μm, diffusion temperature 1020 °C, diffusion time 9 h, waveguide length 40 mm, X-cut and *z* propagation. Offsets: longitudinal offset l_x as indicated on the graph (in millimetres) and lateral offset $l_y = 0.25$ mm (except for the reference guide).

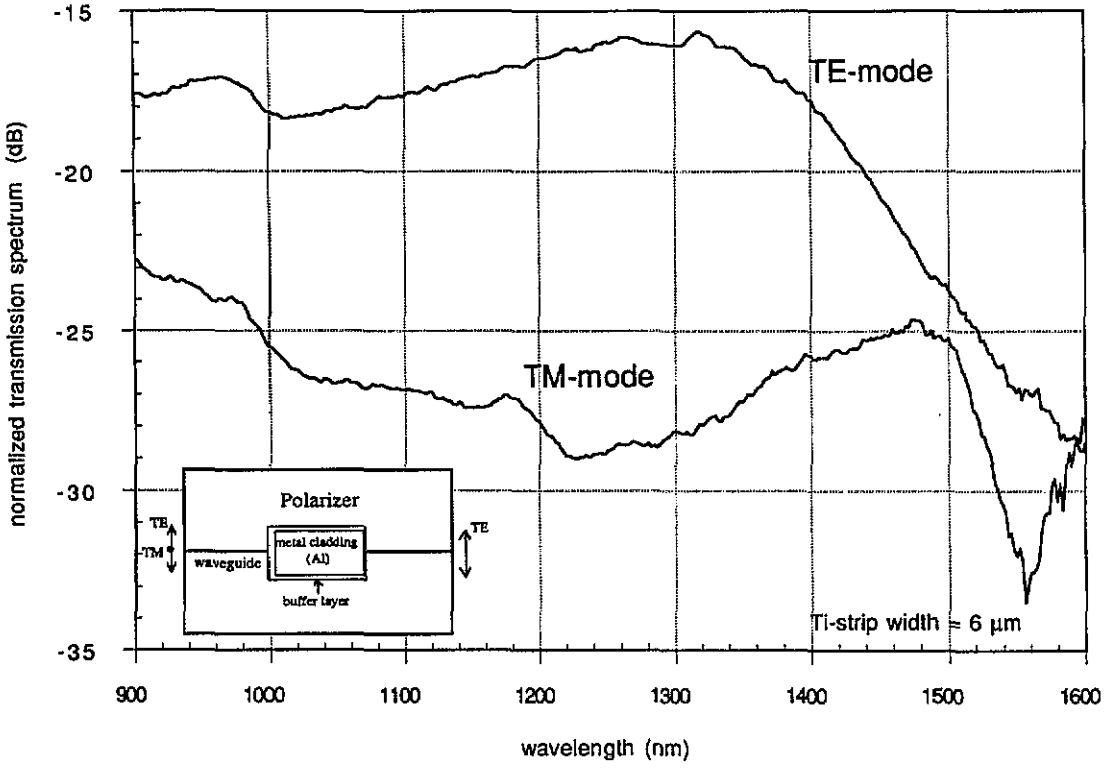

Figure 6. Transmission spectrum and waveguide pattern of a polarizer (for both mode excitations). Fabrication parameters are Ti thickness 650 Å, Ti strip waveguide width 6 μm, diffusion temperature 1015 °C, diffusion time 9 h, waveguide length 16.5 mm, Al cladding length 3 mm, X-cut and *y* propagation.

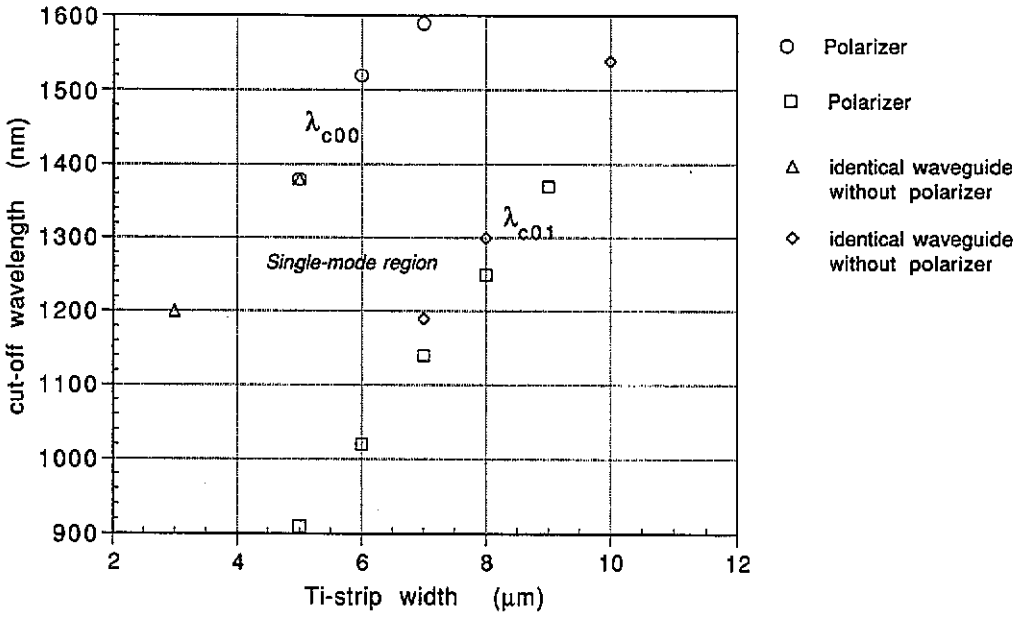

Figure 7. Cut-off wavelengths of polarizers compared to identical waveguides without polarizers. Fabrication parameters are Ti thickness 850 Å, diffusion temperature 1015 °C, diffusion time 9 h, waveguide length 16.5 mm, X-cut, *y* propagation and Al cladding length of the polarizers 6 mm.

The spectral behaviour for TM mode excitation is obviously quite different. Throughout the wavelength range, there is a higher power extinction rate relative to that of the TE mode. It can also be seen that we got an absorption peak for this waveguide (width 6 μm) at $\lambda =$ 1550 nm, which indicates that resonant coupling of the guided wave into the surface plasmon mode takes place at this wavelength. By varying the buffer thickness, the resonant coupling phenomena can be shifted into the operating wavelength and thus the highest extinction ratio of the polarizer can be obtained.

The dependence of the wavelength for resonant coupling as a function of the waveguide width was also verified. For waveguide strip widths of 5 and 7 μm, the wavelengths for resonant coupling were 1480 and 1600 nm respectively.

Compared with straight waveguides of identical fabrication conditions, it could be noted that the cut-off wavelengths of the polarizers for TE mode excitation revealed identical cut-off values or were shifted sometimes to slightly shorter wavelengths (to a maximum of $\Delta\lambda = 50$ nm, see figure 7).

The single-mode guiding region of all the measured channel waveguides or polarizers except the bent waveguides was about 400–500 nm wide. This could not always be achieved with the bent waveguides, for which the single-mode region was slightly reduced by decreasing their curvature radii.

4. Conclusion

An experimental set-up for spectral measurements of integrated optical waveguides was presented, which enables determination of cut-off wavelengths of Ti:$LiNbO_3$ channel waveguides, polarizers and bent waveguides. It also provides an interesting insight into the TM mode spectral behaviour of polarizers in delivering their resonant absorption peak.

The measurement repeatability in terms of cut-off position and transmission level was verified. Whilst the cut-off value could be repeated with a precision of 10 nm, the comparison of the spectra for repeated measurements showed a variation of 2 dB of the transmitted spectral power.

Introducing bends led to a downshift of the cut-off wavelengths up to $\Delta\lambda = 200$ nm and to a narrowing of the single-mode region. The cut-off wavelength of the polarizers for TE mode excitation showed a maximum shift in the cut-off wavelengths of $\Delta\lambda = 50$ nm to shorter wavelengths compared with the corresponding waveguides without polarizers.

Acknowledgments

This work was carried out within the Eureka project EU 458 and supported by the Swiss Government (CERS), the CREE, Orbisphère Laboratories, Haefely (Switzerland) and Thomson Sintra (France), who also supplied the $LiNbO_3$ components.

References

[1] Najafi S I 1992 *Introduction to Glass Integrated Optics* (Norwood, MA: Artech House)

[2] Kitayama Y and Tanaka S 1985 Length dependence of LP_{11} mode cutoff and its influence on the chromatic

dispersion measurements by phase shift method *Proc. SPIE* **584** 229–34
[3] Kitayama K-I, Ohashi M and Ishida Y 1984 Length dependence of effective cutoff wavelength in single-mode fibers *J. Lightwave Technol* **2** 629–33
[4] Cancellieri G and Orfei A 1985 Effective cut-off condition in single-mode optical fibers *Proc. IOOC-ECOC '85* pp 659–62
[5] Coppa G, Costa B, Di Vita P and Rossi U 1985 Cut-off wavelength and mode-field diameter measurements in single-mode fibers *Proc. SPIE* **584** 210–14
[6] 1984 *Characteristics of Single-Mode Optical Fibre Cable* CCITT Recommendation G.652 (Geneva: International Telegraph and Telephone Consultative Committee)
[7] Thyagarajan K, Enard A, Kayoun P, Papillon D and Papuchon M 1985 Measurement of guided mode cut-off wavelengths in Ti: $LiNbO_3$ channel waveguides *European Conf. On Integrated Optics, ECIO '85* pp 236–9
[8] Lamouche G and Najafi S I 1990 Scalar finite-element evaluation of cut-off wavelength in glass wave guides and comparison with experiment *Can. J. Phys.* **68** 1251–6
[9] Minford W J, Korotky S K and Alferness R C 1982 Low-loss Ti: $LiNbO_3$ waveguide bends at $\lambda = 1.3$ μm *IEEE J. Quant. Electron* **18** 1802–6
[10] Polky J N and Mitchell G G L 1974 Metal-clad planar dielectric waveguide for integrated optics *J. Opt. Soc. Am.* **64** 274–9